Aerosol and Air Quality Research, 14: 1017–1027, 2014

ISSN: 1680-8584 print / 2071-1409 online
doi: 10.4209/aaqr.2013.01.0027

Chemical Characterizations of PM_{10} Profiles for Major Emission Sources in Xining, Northwestern China

Jinbao Han[1], Bin Han[2], Penghui Li[1,4], Shaofei Kong[1], Zhipeng Bai[2*], Dehui Han[3], Xiaoyan Dou[3], Xudong Zhao[3]

[1] *College of Environmental Science and Engineering, Nankai University, Tianjin 300071, China*
[2] *Chinese Research Academy of Environmental Sciences, Beijing 100012, China*
[3] *Qinghai Environmental Monitoring Center, Xining, Qinghai 810007, China*
[4] *Environmental Science and Safety Engineering, Tianjin University of Technology, Tianjin 300191, China*

ABSTRACT

The chemical profiles of emission sources are indispensable for source apportionment using receptor models. To develop current knowledge of PM_{10} profiles, the chemical composition of major emission sources were analyzed in Xining. Samples of geological sources (soil dust, road dust and construction derived dust) and industrial fly ash were collected from representative portions using a plastic dustpan and brush and sampled on filters through a re-suspension chamber. Samples of coal combustion source and vehicle exhaust were collected directly on the filters using a dilution stack sampler. Chemical analysis included inductively coupled plasma mass spectrometry for 19 elements (Na, P, K, As, Rb, Mo, Cd, Sn, Sb, La, V, Cr, Mn, Co, Ni, Cu, Zn, T1, and Pb), inductively coupled plasma optical emission spectrometry for 7 elements (Al, Sr, Mg, Ti, Ca, Fe, and Si), ion chromatography for water-soluble ions (Na^+, K^+, Mg^{2+}, Ca^{2+}, F^-, Cl^-, NO_3^- and SO_4^{2-}) and thermal/optical reflectance analysis for carbonaceous species.

Crustal elements (Si, Al, Ca, Fe) predominated in geological sources, whereas trace elements (Pb, Cd, Cr, Zn and Ni) were predominant in industrial fly ash. An abundance of carbon and SO_4^{2-} was present in coal-combustion source and vehicle exhaust. The coal-combustion boilers were a source of trace elements (Ti, Co, Sr, Sb, Tl). High concentrations of Pb and OC in soil indicated the strong influence of agriculture activities in Xining. Comparison of vehicle exhaust profiles indicated that natural gas was high environmental friendliness in comparison with petroleum products used as motor vehicles fuel. Differences in EC, Cd and NO_3^- between natural gas-powered and gasoline- or diesel-powered vehicle exhaust can be used to differentiate the two types of vehicle emission sources. Differences in source profiles and indicator species between Xining and other cities suggest that source profiles should be developed locally and updated frequently.

Keywords: PM_{10}; Source profiles; Chemical species; Indicator species; Source apportionment; Air pollution.

INTRODUCTION

Source apportionment using receptor models, one of the main methods used to quantify contributions of different sources to atmospheric particulate matter (PM), is well established and widely used (Watson *et al.*, 2002; Samara *et al.*, 2003; Gupta *et al.*, 2007). It requires information about the chemical characteristics of the emission sources that affect pollutant concentrations at a receptor (Watson and Chow, 2001). Hundreds of PM chemical source profiles have been compiled and used in source apportionment studies (Ning *et al.*, 1996; Chow *et al.*, 2004; Watson *et al.*, 2001; Aldabe *et al.*, 2011). However, these source profiles differ with respect to geographical location and time (Ning *et al.*, 1996; Li *et al.*, 2001; Thorpe and Harrison, 2008). It is therefore preferable to use the most recent local profiles for source apportionment studies (Paode *et al.*, 1999). Inhalable particles (PM_{10}, particulate matter with aerodynamic diameters less than 10 μm) is the most significant air pollutant in China (Ning *et al.*, 1996; Zhao *et al.*, 2006; Bi *et al.*, 2007; Han *et al.*, 2009; Zhang *et al.*, 2010) and determining how to meet the PM_{10} air quality standard remains a challenge for Chinese central and local environmental management agencies. Considerable efforts have been made to study the chemical source profiles of PM_{10} across China. However, these studies mainly focused on the developed cities in eastern and southern China such as Beijing (Han *et al.*, 2007; Shoubin *et al.*, 2009; Chen *et al.*, 2010), Tianjin (Li and Bai, 2009; Kong *et al.*, 2010), Shanghai (Waheed *et al.*, 2011), Hongkong (Ho *et al.*, 2003) etc. With urbanization

* Corresponding author.
Tel.: 86-10-8491-5246; Fax: 86-22-2350-3397
E-mail address: zbai@nankai.edu.cn

and development in western China, air quality in some western Chinese cities is rapidly deteriorating.

Xining, the capital of Qinghai province of China, is the biggest city of the Qinghai-Tibetan plateau and is situated at the eastern entrance into the Qinghai-Tibetan plateau. For the past two decades, due to increasing emissions from vehicles, factories and domestic heating, the air of Xining has been heavily polluted. The urban area of Xining is surrounded by mountains on all sides, so air stagnation is commonplace. According to China Statistical Yearbook of 2011 (National Bureau of Statistics of China, 2011), Xining had the 4th worst air quality (annual mean PM_{10} of 124 μg/m^3) among 31 major cities of China in 2010, and was worse than Beijing (annual mean PM_{10} of 121 μg/m^3). However, because information on source emissions, especially the chemical composition in PM_{10} has not been available, it is difficult to conduct a source apportionment and put forward effective air pollution control strategies. It is therefore important to obtain PM_{10} chemical profiles for major emission sources in Xining.

This is the first study on chemical characterization of PM_{10} source profiles of major emission sources in Xining. The objective is to develop current knowledge of PM_{10} chemical source profiles for geological material, industrial fly ash, coal-fired boiler emissions and motor vehicle exhaust in order to construct emission inventories and apportion ambient concentrations to sources using receptor modeling for the ultimate purpose of guiding the pollution control efforts.

METHODOLOGY

Study Area

Xining (101°49′17″E, 36°34′3″N) is located on the eastern edge of the Tibetan Plateau and the upstream area of the Huangshui River. The elevation of the city is 2, 295 m above sea level. The city is characterized by a plateau mountain climate. The annual average precipitation is 380 mm and average temperature is 7.6°C. The city has a population of more than two million, and includes residents of 37 nationalities. Governance of Xining includes five districts, three counties and one national economic and technological development zone. Manufacture of aluminum, iron and steel, production of cement and metallurgy are the major industries in Xining, and economic growth is rapid.

Sampling and Pre-treatment

The potential sources that contribute to PM concentrations in Xining were identified based on observations and available emission inventories. A total of 94 samples were collected in and around the urban areas in 2010. Table 1 summarizes the emission source samples taken in this study.

The dust samples included soil dust (SD), road dust (RD), construction dust (CD) and industrial fly ash were collected from representative portions using a plastic dustpan and brush for about 1 kg and then transferred into coded valve bags. Any obvious material was not collected. Each spatula and brush was used once before giving a thorough cleaning. Coordinates of the sample locations (shown in Fig. 1) were obtained with a GPS.

Dust samples were pre-treated using a re-suspension chamber to collected PM_{10}. Each sample was dried in a vacuum freeze dryer and then weighed and sieved through a 160-mesh Tyler screen to remove fibers and other larger particles. Approximately 0.5 g of sieved material was then placed in a 250 mL sidearm vacuum flask sealed with a rubber stopper. Clean air puffs into the flask blew the dust into a chamber. The dust was then deposited onto filters through PM_{10} inlets at a flow rate of 20 L/min for approximately 1 min (Kong *et al.*, 2011a, c). Polypropylene membrane filters (Pall, Φ 47 mm) and quartz fiber filters (Pall, Φ 47mm) were used on two parallel channels during dust re-suspension.

For the coal combustion and motor vehicle exhaust sources, the PM_{10} samples were collected directly onto the filters using a dilution stack sampler (Chow *et al.*, 2004). Five coal-fired boiler samples were obtained from the main plants in Xining including an electrical generating plant that supplied power for domestic use and two plants that supplied power to an aluminum processing facility and an iron and steel manufacturing plant. Twelve motor vehicle exhaust samples were obtained from the exhaust pipes of the main vehicle types in Xining including a bus and a taxi

Table 1. Descriptions of sampling data of PM_{10} profiles for major emission sources in Xining.

Source type	Abbr.	Descriptions	Num.
Soil dust	SD	Topsoil (between ground surface layer and 1–20 cm below) soils around the city including orchard, cropland, wasteland, dry lake bed and urban parks	22
Road dust	RD	Dust from the crossroads of main roads and entrance of highway in the urban district	25
Construction derived dust	CD	Dust samples from the surfaces of windowsills, flat roofs and stairs at building sites	7
	CP	Cement production samples from major cement plants and construction sites located in and around the urban areas	6
Industrial fly ash	SFA	Fly ash from dust control devices of a silicon plant	3
	EAFA	Fly ash from the workshop and the flue pipe of a precipitator in an electrolytic aluminum plant	3
	ISFA	Fly ash from dust control devices of an iron and steel smelt plant	11
Coal combustion sources	CFA	Fly ash from domestic and industrial coal-fired boilers	5
Motor vehicle exhaust	GFVE	Samples from exhaust pipes of natural gas-powered bus and taxi	6
	OFVE	Samples from exhaust pipes of diesel-powered truck and gasoline-powered taxi	6

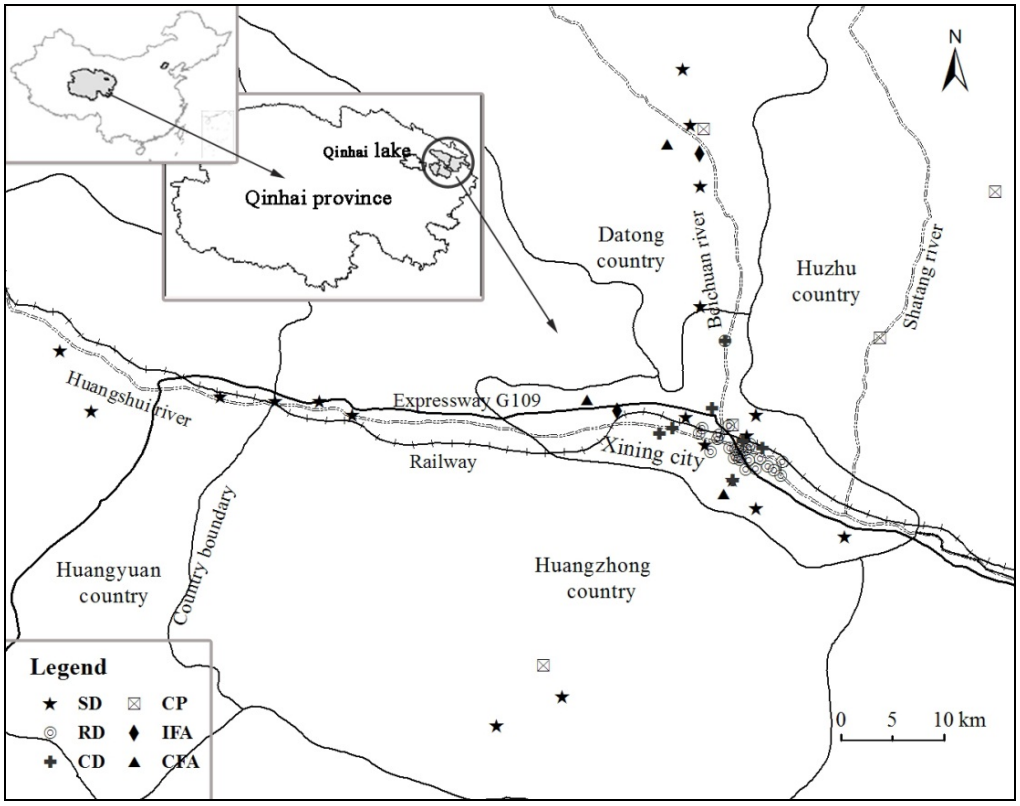

Fig. 1. Sampling sites for major emission sources in Xining (SD: soil dust; RD: road dust; CD: construction dust; CP: cement production; IFA: industrial fly ash; CFA: coal-burning fly ash).

using natural gas which contains sulfur below 200 mg/m^3 as fuel, a truck using diesel oil which contains sulfur below 350 ppm and a taxi using gasoline which contains sulfur below 150 ppm as fuel. During the period of sampling, the bus made round trips from the origin to the terminus of the bus line, and the passengers got on and off as usual. The taxi traveled around the city as usual. The truck traveled in two stages, one full-load and one zero-load, with sampling performed three times for each stage.

The polypropylene and quartz-fiber filters were calcined at 60 ± 1°C for 0.5 h and at 800 ± 1°C for 2 h, respectively, to remove any organic compounds before sampling. After sampling, the filters were removed from the inlets and placed in a clean petri dish until used. Filters were equilibrated at a relative humidity (35 ± 1%) and temperature (22.0 ± 1°C) controlled environment for 72 h before gravimetric analysis to minimize particle volatilization and aerosol liquid water bias. Filters were exposed to a low-level radioactive source prior to weighing to remove static charge and weighed both before and after sampling using a sensitive microbalance (Mettler M5, ± 0.001 mg). After weighing, the filters were stored at –4°C pending chemical analysis (Kong *et al.*, 2011b). Filter blanks were treated in the same manner. All procedures were quality controlled strictly to avoid possible sample contamination.

Chemical Analysis

PM_{10} concentrations were obtained using standard gravimetric methods. For elemental analysis, half of each polypropylene filter with PM_{10} was analyzed for 19 elements including sodium (Na), phosphorus (P), potassium (K), arsenic (As), rubidium (Rb), molybdenum (Mo), cadmium (Cd), stannum (Sn), antimony (Sb), lanthanum (La), vanadium (V), chromium (Cr), manganese (Mn), cobalt (Co), nickel (Ni), copper (Cu), zinc (Zn), thallium (T1), and lead (Pb) by inductively coupled plasma mass spectrometry (ICP-MS; Agilent 7500a, Agilent Co., USA). The other half was analyzed for 7 elements including aluminum (Al), strontium (Sr), magnesium (Mg), titanium (Ti), calcium (Ca), iron (Fe), and silicon (Si) by inductively coupled plasma optical emission spectrometry (ICP-OES; IRIS Intrepid II, Thermo Electron Co., USA). For ICP-MS, each polypropylene filter was cut into pieces and placed into a 100 mL polyfluortetraethylene beaker with 5 mL HNO_3 (pH = 5.6) and a drop of HF (pH = 5.3) was added. After covering, the solution was heated on a hot plate at 220°C for 2.5 h. Then the hot plate was turned off and 5 mL HCl was added to the solution which was then transferred into a 10 mL plastic bottle. Finally, the digested samples were diluted to 10 mL with deionized water (Kong *et al.*, 2011a; Kong *et al.*, 2012). For ICP-OES, each polypropylene filter piece was ashed in a nickel crucible at 300°C for 40 minutes and then at 540°C in a muffle furnace. The samples were then cooled and several drops of anhydrous alcohol were added and melted at 500°C for 10 minutes with 0.2 g sodium hydroxide. After cooling, the solution was transferred into a plastic tube pre-filled with 2 mL HCl solution. The crucible was flushed with 2% of HCl and the rinse solution

was transferred into the tube. Finally, the digested samples were diluted to 10 mL with deionized water (Kong *et al.*, 2011a, 2012).

An eighth of each quartz filter with PM_{10} was used for ion analysis including sodion (Na^+), soluble potassium (K^+), soluble magnesium (Mg^{2+}), soluble calcium (Ca^{2+}), fluoride (F^-), chloride (Cl^-), nitrate (NO_3^-) and sulfate (SO_4^{2-}). These were cut into pieces into a vessel with scale and extracted with 5 mL deionized water in an ultrasonic cleaner (Type AS3120A, AutoScience Inc.) at a frequency of 40 kHz for 15 min. One milliliter of the extracts was drawn into a syringe, filtrated twice using a 13 mm cellulose syringe filter with a 0.22 μm of pore size, and injected into an ion chromatograph (IC; Dionex DX-120, Dionex Ltd., USA) consisting of a separation column (CS12A for cations and AS14 for anions) and a guard column (CG12A for cations and AG14 for anions). Methanesulfonic acid (20 mmol/L) at a flow rate of 1.0 mL/min was used as an eluent for cation detection and a mixture of Na_2CO_3 (3.5 mmol/L) and $NaHCO_3$ (1.0 mmol/L) at a flow rate of 1.2 mL/min was used for anion detection.

The remaining part of each quartz filter was punched and analyzed for organic carbon (OC), elemental carbon (EC) and total carbon (TC) by thermal/optical reflectance (TOR) analysis following the Interagency Monitoring of Protected Visual Environments (IMPROVE) protocol using a DRI Model 2001 Thermal/Optical Carbon Analyzer (Atmoslytic Inc., USA). Following the protocol, the punch aliquot (0.521 cm^2) was heated stepwise at temperatures of 120°C (OC1), 250°C (OC2), 450°C (OC3), and 550°C (OC4) in a non-oxidizing helium (He) atmosphere, and 550°C (EC1), 700°C (EC2), and 800°C (EC3) in an oxidizing atmosphere (helium with 2% oxygen). The carbon that evolved at each temperature was oxidized to carbon dioxide (CO_2), and then reduced to methane (CH_4) for quantification using a flame ionization detector. As temperature increased in the inert helium, some of OC pyrolyzed to EC, resulting in darkening of the filter deposit that was monitored by reflectance of 633 nm light from a He-Ne laser. When oxygen was added, the original and pyrolyzed EC combusted and resulting in an increase in reflectance. The amount of carbon measured after oxygen was added until the reflectance reached its original value was recorded as optically detected pyrolyzed carbon (OPC). The eight fractions (OC1, OC2, OC3, OC4, EC1, EC2, EC3, and OPC) were recorded separately. The IMPROVE protocol defines the following: OC = OC1 + OC2 + OC3 + OC4 + OPC, EC = EC1 + EC2 + EC3 – OPC and TC = OC + EC (Li *et al.*, 2012).

Quality Assurance and Quality Control

Each filter was weighed three times before and after sampling and the three readings were averaged. All procedures were strictly controlled to avoid contamination of the samples.

For elemental analysis, geochemistry reference material GBW07402 from the National Research Center of Reference Materials was analyzed to evaluate the accuracy of ICP-MS, GBW07401, GBW07404 and GBW07406 were used to check the reliability of ICP-OES. The method detection limits (MDLs) were 0.0764 μg/mL for Na, 0.0023 μg/mL for P, 0.1027 μg/mL for K, 0.0014 μg/mL for As, 0.0005 μg/mL for Rb, 0.0001 μg/mL for Mo, 0.0003 μg/mL for Cd, 0.0001 μg/mL for Sn, 0.0001 μg/mL for Sb, 0.0004 μg/mL for La, 0.0002 μg/mL for V, 0.0017 μg/mL for Cr, 0.0009 μg/mL for Mn, 0.00004 μg/mL for Co, 0.0009 μg/mL for Ni, 0.0026 μg/mL for Cu, 0.0114 μg/mL for Zn, 0.00001 μg/mL for T1, 0.0005 μg/mL for Pb, 0.045 μg/mL for Al, 0.004 μg/mL for Sr, 0.047 μg/mL for Mg, 0.024 μg/mL for Ti, 0.039 μg/mL for Ca, 0.181 μg/mL for Fe, and 0.069 μg/mL for Si. Background contamination was routinely monitored by using operational blanks that were processed simultaneously with field samples. One standard sample was analyzed per ten field samples to assure that percent recovery was in the range of 80%–120%. One sample in ten was analyzed twice, relative error was less than 20%.

For ion analysis, standard solutions were prepared and were analyzed three times. Results showed that the relative standard deviations for Na^+, K^+, Mg^{2+}, Ca^{2+}, F^-, Cl^-, NO_3^- and SO_4^{2-} were 0.25%, 0.09%, 0.47%, 0.49%, 0.18%, 0.18%, 2.37% and 0.71%, respectively, and MDLs were 0.2864 mg/L, 0.1229 mg/L, 0.063 mg/L, 0.198 mg/L, 0.0342 mg/L, 0.2556 mg/L, 2.387 mg/L and 6.6816 mg/L, respectively.

For carbon component analysis, the analyzer was calibrated with known quantities of CH_4 daily. Replicate analyses were performed on one of every 10 samples. Standard sample was analyzed twice weekly, percent recovery was in the range of 98%–102%. Analytical detection limits were obtained using blank filters processed in an identical manner as the samples. Typical MDLs for OC, EC and TC were 0.82 μg/cm^2, 0.19 μg/cm^2 and 0.93 μg/cm^2, respectively.

RESULTS AND DISCUSSION

The profile for each source type was derived by averaging the profiles from individual samples. Table 2 shows the average abundance (weight percent by mass) and standard deviations of all of the analysed species for each of the source profiles discussed below.

Soil Dust (SD)

The elements as a group were the main contributors to soil dust PM_{10} mass, accounting for 39.0% of the mass; most of the elemental contribution, as a expected, was due to crustal components such as Si (17.02%), Al (6.89%), Ca (5.91%) and Fe (3.88%). Ca^{2+} (3.85 %), Na^+ (0.91%) and SO_4^{2-} (0.64%) were the major water-soluble ion species, with the abundance in the ranges of 1.03-8.81%, 0.34-4.20% and 0.18-0.97%, respectively. There are similar to ranges reported in other studies (Watson and Chow, 2001; Cao *et al.*, 2008; Kong *et al.*, 2011a). The low standard deviation for abundance of species in soil dust suggested that different soil dust samples were similar.

The Ca/Al ratio was used as a marker of Asian dust (Cao *et al.*, 2008; VanCuren and Cahill, 2002). Ca/Al ratios in this study ranged from 0.60 to 1.27, comparable to those in other sources of Asian dust (0.74-2.7) (Watson and Chow, 2001; Cao *et al.*, 2008; Kong *et al.*, 2011a). Because Xining is located in the bordering area of the Qinghai-Tibet plateau

Table 2. Chemical composition (weight percent by mass, %) of PM_{10} profiles for major emission sources in Xining.

	SD	RD	CD	CP	SFA	EAFA	ISFA	CFA	GFVE	OFVE
Na	0.67 ± 0.13	0.84 ± 0.24	0.68 ± 0.13	0.43 ± 0.10	0.85 ± 0.39	1.81 ± 0.16	0.66 ± 0.46	0.52 ± 0.48	0.51 ± 0.16	0.81 ± 0.64
Mg	1.55 ± 0.28	1.71 ± 0.39	1.49 ± 0.71	0.94 ± 0.25	1.03 ± 0.24	0.25 ± 0.19	0.54 ± 0.44	0.69 ± 0.24	0.33 ± 0.25	0.63 ± 0.70
Al	6.89 ± 0.61	5.16 ± 0.62	6.60 ± 1.82	5.13 ± 0.38	5.21 ± 1.56	24.52 ± 3.97	3.06 ± 4.64	1.39 ± 1.27	3.86 ± 1.66	5.45 ± 3.43
Si	17.01 ± 1.62	12.47 ± 1.56	14.32 ± 5.11	9.80 ± 1.36	17.40 ± 2.96	3.24 ± 2.99	2.61 ± 1.54	2.46 ± 1.67	3.30 ± 2.00	2.39 ± 1.30
P	0.14 ± 0.06	0.11 ± 0.03	0.10 ± 0.01	0.06 ± 0.02	0.10 ± 0.04	0.03 ± 0.03	0.07 ± 0.01	0.12 ± 0.05	0.07 ± 0.08	0.05 ± 0.05
K	2.33 ± 0.17	1.55 ± 0.17	1.85 ± 0.37	1.01 ± 0.13	1.65 ± 0.49	1.02 ± 0.45	1.70 ± 1.02	0.54 ± 0.50	0.31 ± 0.11	0.55 ± 0.34
Ca	5.91 ± 0.78	9.84 ± 2.33	9.31 ± 3.15	13.66 ± 2.67	7.56 ± 2.49	1.01 ± 0.92	7.16 ± 4.11	6.15 ± 2.79	1.75 ± 1.23	1.18 ± 0.88
Ti	0.29 ± 0.03	0.26 ± 0.05	0.27 ± 0.10	0.21 ± 0.04	0.23 ± 0.04	0.05 ± 0.05	0.09 ± 0.06	2.06 ± 2.59	0.09 ± 0.05	0.04 ± 0.03
V	0.01 ± 0.00	0.01 ± 0.00	0.01 ± 0.00	0.01 ± 0.00	0.01 ± 0.00	0.00 ± 0.00	0.01 ± 0.00	0.01 ± 0.00	0.00 ± 0.00	0.00 ± 0.00
Cr	0.01 ± 0.00	0.02 ± 0.01	0.01 ± 0.00	0.04 ± 0.03	0.03 ± 0.01	0.01 ± 0.00	0.02 ± 0.00	0.03 ± 0.05	0.03 ± 0.04	0.04 ± 0.02
Mn	0.09 ± 0.01	0.08 ± 0.01	0.08 ± 0.01	0.07 ± 0.02	0.11 ± 0.03	0.02 ± 0.01	0.15 ± 0.03	0.07 ± 0.02	0.04 ± 0.03	0.12 ± 0.11
Fe	3.88 ± 1.01	2.74 ± 0.49	2.90 ± 1.00	1.69 ± 0.21	4.51 ± 1.22	0.93 ± 0.67	28.29 ± 12.08	1.55 ± 1.54	0.71 ± 0.50	0.82 ± 0.67
Co	0.00 ± 0.00	0.00 ± 0.00	0.00 ± 0.00	0.00 ± 0.00	0.00 ± 0.00	0.00 ± 0.00	0.00 ± 0.00	0.07 ± 0.10	0.00 ± 0.00	0.00 ± 0.00
Ni	0.01 ± 0.00	0.01 ± 0.01	0.00 ± 0.00	0.01 ± 0.00	0.04 ± 0.02	0.09 ± 0.03	0.02 ± 0.04	0.01 ± 0.00	0.06 ± 0.05	0.07 ± 0.07
Cu	0.02 ± 0.01	0.03 ± 0.04	0.01 ± 0.00	0.01 ± 0.01	0.03 ± 0.01	0.01 ± 0.00	0.03 ± 0.02	0.01 ± 0.01	0.14 ± 0.08	0.46 ± 0.41
Zn	0.07 ± 0.01	0.10 ± 0.08	0.03 ± 0.01	0.02 ± 0.01	0.23 ± 0.07	0.03 ± 0.02	0.26 ± 0.10	0.25 ± 0.29	0.16 ± 0.12	0.48 ± 0.32
As	0.00 ± 0.00	0.00 ± 0.00	0.00 ± 0.00	0.00 ± 0.00	0.00 ± 0.00	0.01 ± 0.00	0.00 ± 0.00	0.00 ± 0.00	0.01 ± 0.00	0.01 ± 0.01
Rb	0.01 ± 0.00	0.01 ± 0.00	0.01 ± 0.00	0.01 ± 0.00	0.01 ± 0.00	0.00 ± 0.00	0.02 ± 0.02	0.01 ± 0.01	0.00 ± 0.00	0.00 ± 0.00
Sr	0.03 ± 0.01	0.03 ± 0.00	0.04 ± 0.01	0.03 ± 0.01	0.03 ± 0.01	0.01 ± 0.00	0.01 ± 0.01	0.68 ± 0.83	0.00 ± 0.00	0.00 ± 0.01
Mo	0.00 ± 0.00	0.00 ± 0.00	0.00 ± 0.00	0.00 ± 0.00	0.00 ± 0.00	0.00 ± 0.00	0.00 ± 0.00	0.00 ± 0.00	0.01 ± 0.01	0.01 ± 0.00
Cd	0.00 ± 0.00	0.00 ± 0.00	0.00 ± 0.00	0.00 ± 0.00	0.00 ± 0.00	0.00 ± 0.00	0.00 ± 0.00	0.01 ± 0.01	0.00 ± 0.00	0.00 ± 0.00
Sn	0.00 ± 0.00	0.00 ± 0.00	0.00 ± 0.00	0.00 ± 0.00	0.01 ± 0.00	0.00 ± 0.00	0.01 ± 0.01	0.00 ± 0.00	0.00 ± 0.00	0.01 ± 0.01
Sb	0.00 ± 0.00	0.00 ± 0.00	0.01 ± 0.02	0.00 ± 0.00	0.00 ± 0.00	0.00 ± 0.00	0.00 ± 0.00	0.00 ± 0.00	0.00 ± 0.00	0.00 ± 0.00
La	0.00 ± 0.00	0.00 ± 0.00	0.00 ± 0.00	0.00 ± 0.00	0.00 ± 0.00	0.00 ± 0.00	0.00 ± 0.00	0.00 ± 0.00	0.00 ± 0.00	0.00 ± 0.00
Tl	0.00 ± 0.00	0.00 ± 0.00	0.00 ± 0.00	0.00 ± 0.00	0.00 ± 0.00	0.00 ± 0.00	0.00 ± 0.00	0.00 ± 0.00	0.00 ± 0.00	0.00 ± 0.00
Pb	0.08 ± 0.07	0.03 ± 0.01	0.01 ± 0.00	0.01 ± 0.00	0.05 ± 0.02	0.03 ± 0.02	1.02 ± 0.81	0.11 ± 0.07	0.04 ± 0.03	0.03 ± 0.01
Na^+	0.91 ± 0.85	1.06 ± 0.63	0.86 ± 0.61	0.57 ± 0.27	3.05 ± 1.86	2.19 ± 0.33	1.78 ± 1.70	1.01 ± 1.18	7.40 ± 5.75	9.38 ± 6.85
K^+	0.31 ± 0.21	0.65 ± 0.32	0.35 ± 0.17	0.31 ± 0.15	0.73 ± 0.13	0.44 ± 0.03	0.44 ± 0.39	0.14 ± 0.16	-	-
Mg^{2+}	0.19 ± 0.13	0.41 ± 0.18	0.22 ± 0.10	0.19 ± 0.09	0.45 ± 0.08	0.27 ± 0.02	0.27 ± 0.24	0.22 ± 0.23	0.63 ± 1.02	1.41 ± 0.80
Ca^{2+}	3.85 ± 2.02	6.02 ± 2.41	3.26 ± 0.89	1.82 ± 0.64	7.50 ± 2.48	1.38 ± 0.55	5.82 ± 3.87	2.69 ± 2.01	3.71 ± 5.85	7.59 ± 4.33
F^-	0.05 ± 0.04	0.02 ± 0.01	0.02 ± 0.01	0.03 ± 0.03	0.07 ± 0.04	2.20 ± 1.94	0.32 ± 0.43	0.32 ± 0.17	0.31 ± 0.35	0.65 ± 1.14
Cl^-	0.40 ± 0.23	0.18 ± 0.06	0.18 ± 0.05	0.05 ± 0.02	0.33 ± 0.12	0.15 ± 0.02	2.18 ± 2.17	1.78 ± 1.15	0.47 ± 0.40	1.30 ± 1.28
NO_3^-	0.04 ± 0.02	0.06 ± 0.06	0.00 ± 0.01	-	-	-	-	0.13 ± 0.16	0.34 ± 0.32	1.81 ± 2.51
SO_4^{2-}	0.64 ± 0.29	1.38 ± 0.83	0.99 ± 0.61	5.34 ± 2.82	2.57 ± 2.10	1.55 ± 0.44	2.88 ± 1.58	6.93 ± 4.05	6.09 ± 6.68	8.01 ± 9.20
TC	3.09 ± 0.41	6.58 ± 1.94	3.35 ± 1.35	2.15 ± 0.74	7.03 ± 1.79	4.74 ± 2.55	2.91 ± 1.51	19.90 ± 7.44	46.17 ± 20.04	41.52 ± 9.90
OC	3.04 ± 0.47	5.98 ± 1.86	3.15 ± 1.23	1.35 ± 0.49	4.44 ± 1.68	0.99 ± 0.51	2.45 ± 0.90	11.03 ± 5.13	43.78 ± 18.91	22.75 ± 8.77
EC	0.10 ± 0.16	0.60 ± 0.13	0.35 ± 0.18	0.80 ± 0.44	2.59 ± 0.21	3.75 ± 2.48	0.46 ± 0.97	8.87 ± 2.80	2.38 ± 1.73	18.78 ± 12.17

Note: dashes indicate values that were not detected.

and loess plateau, the ratios of Si/Al and Mn/Al of 2.47 (from 2.20 to 2.66) and 0.014 (from 0.01 to 0.18), respectively, for soil dust this study were similar to 3.0 and 0.012 reported previously for Chinese loess plateau soil dust (Cao *et al.*, 2008). The Pb abundance was 0.08%, nearly 3 times higher than that in either road dust or the background value of Qinghai province (Ministry of Environmental Protection of China, 1990). This could be attributed to crop debris and the use of pesticides, animal manures and fertilizers (Atafar *et al.*, 2010) or wastewater irrigation (Wei *et al.*, 2009).

The abundances of OC and EC were 3.04% and 0.06%, respectively. OC/TC ratios for different geological source profiles have shown substantial variation (Chow *et al.*, 1994). In this study, the average OC/TC ratio was 0.98, which is similar to that in Imperial and Mexicali Valleys along the California/Mexico border (Watson and Chow, 2001), but approximately 70% higher than the corresponding ratio in Fushun (Kong *et al.*, 2011a). This difference is due to the large number of agricultural activities in Xining, while coal mining is a dominant industry in Fushun. Crop debris and agricultural chemicals, including pesticides, herbicides and fertilizers might contribute to the OC abundance in Xining (Cao *et al.*, 2008).

Road Dust (RD)

Similar to the source profile of soil dust, the road dust profile contained the most abundant species of Si, Ca, Al, Fe, Ca^{2+} and SO_4^{2-}, with values of 12.47%, 9.84%, 5.16%, 2.74%, 6.02% and 1.38%, respectively (Table 2). However, the trace elements (Cr, Ni, Cu, Zn, Cd, Sn, Sb) and carbonaceous species (OC, EC) of RD were more prominent than those in SD, indicating that RD contains a mixture of geological material, industrial emissions and vehicle emissions (Watson and Chow, 2001). The content of Zn in RD was was 55% higher than the corresponding content in SD, indicating Zn in RD is a reflection of tire wear (Ho *et al.*, 2003) because of the use of a vulcanization agent in vehicle tires (Fergusson and Kim, 1991). However, Zn concentration of RD in this study was 80% lower than in RD in Hong Kong (Ho *et al.*, 2003). This could be attributed to the low temperature of the plateau mountain climate in Xining, which results in the lower wear rates of vehicle tires. The concentration of EC in RD was 10 times higher than that in SD, reflecting the effect of traffic and coal combustion. Because EC is regarded as an indicator of incomplete combustion of carbon-containing fuels and the EC concentration in OFVE and CFA was 18.78% and 8.87%, respectively, in Xining. Since Pb was phased out of gasoline, Pb emissions from traffic have decreased greatly, the abundance of Pb in road dust was close to the soil background value in Qinghai province.

Construction Derived Dust

In Xining, because building construction is ongoing at a rapid pace in the urban area, there are substantial emissions from construction derived dust. The most abundant species were Si (14.32%) for CD and Ca (13.66%) for CP, respectively. Other prominent (more than 1%) species include Al, K, Fe, Ca^{2+} and OC for both profiles, as well as Mg and Ca for the CD profile and Si and SO_4^{2-} for the CP profile. Ho *et al.* (2003) and Kong *et al.* (2011a) reported that the major crustal species (Si and Al) were the abundant constituents of construction derived dust. Note that the abundance of Sb in CD was 30 times that in CP reflecting the Sb-containing white paint used in whitewashing rooms (Jha *et al.*, 2009). Comparing with CP, CD was a mixture of cement, sand, brick, paint, dust, and so on, which caused a decrease in the level of SO_4^{2-} (0.99% in CD and 5.34% in CP).

Industrial Fly Ash

The PM_{10} industrial sources profiles from different plants differed from each other due to differences in production processes, combustion processes and pollution control devices. For the SFA profile, Si (17.40%) was the most abundant species, following by Ca (7.56%) and Ca^{2+} (7.50%). Elements of Al (5.21%), Fe (4.51%) and ions of Na^+ (3.05%), SO_4^{2-} (2.57%) were also abundant. The abundances of OC and EC in SFA were 4.44% and 2.59%, respectively. For the EAFA profile, Al (24.52%) was the most abundant element, following by Si (3.24%) and Na (1.81%). F^- (2.20%) was the most abundant ion, following by Na^+ (2.19%) and SO_4^{2-} (1.55%). The abundances of OC and EC in ISFA were 0.99% and 3.75%, respectively. For the ISFA profile, Fe (28.29%), Ca (7.16%) and Ca^{2+} (5.82%) were abundant species. The ISFA profile was also enriched in Al (3.06%), SO_4^{2-} (2.88%) and Si (2.61%). The abundances of OC and EC in ISFA were 2.45% and 0.46%, respectively. The abundance of Si in SFA profile was similar to the profiles of SD, RD and CD, indicating that Si cannot be used as the only indicator element for geological material in Xining. Similar findings were reported by Chow *et al.* (2004), who pointed out that industrial fly ash was dominated by Al, Si, Ca and Fe.

It is important to also consider the contribution of ISFA to concentrations of Sn and Pb at the receptor, since the abundance of these trace elements in ISFA was one to two orders of magnitude higher than that in other source profiles. The EAFS profile contained lower amounts of metallic elements except Ni, As and Sb compared to the SFA and ISFA profiles. Yatkin and Bayram (2008) reported that steel furnaces were major emitters of trace elements such as Pb, Zn, Cd, Cr, and Cu. The abundance of F^- in the EAFS profile was 6 and 31 times higher than that in ISFA and SFA respectively, indicating EAFS was the source of F^-.

Coal Combustion Sources

The coal-fired boiler profile was dominated by OC, EC, SO_4^{2-}, Ca, Si, Fe and Al, with abundances of 11.03%, 8.87%, 6.93%, 6.15%, 2.46%, 1.55% and 1.39%, respectively. This was consistent with the study of Bi *et al.* (2007) in which Si, Ca, Al, Fe, OC and TC were found to be the abundant species for coal combustion fly ash from six northern Chinese cities. The CFA profile was also enriched in Ti, Co, Sr, Cd, Sb and Tl, which were nearly 7-, 37-, 25-, 16-, 6- and 5-times as abundant as in SD respectively, suggesting that coal combustion was the main contributor to these elements. The concentration of semivolatile metals

such as Cd, Sb, Tl and Pb in coal combustion fly ash were obviously different from that in motor vehicle exhaust particles. This could be attributed to different components and combustion temperatures for coal and petroleum products. These metals may vaporize at the high temperature and return to the solid phase as temperature decreases (Davis and Wendt, 2000). The average OC/TC ratio was 0.55 (range 0.46 to 0.62), which is similar to that found in northwestern Colorado (0.56) by Watson *et al.* (2001), but lower than that in the soil dust profile, consistent with the 160-times abundance of EC in the coal-fired source relative to SD.

Motor Vehicle Exhaust

The carbon components were the most abundant species in exhaust emission from either natural gas powered vehicles or petroleum products powered vehicles, accounting for 59.2% and 48.5% of the total mass, respectively. The abundance of OC in GFVE was 43.78%, which was 2-44 times that in other profiles. The abundance of EC in OFVE was 18.78%, which 2-339 times that in other profiles. This is an important observation, since OC and EC can be used as one of the key markers to distinguish GFVE and OFVE from other sources, respectively. Although the OC abundances in GFVE varied from 22.82% to 63.03%, the OC/TC ratios were relatively consistent (from 0.91 to 0.97). The OC/TC ratios in OFVE ranged from 0.34 to 0.87, with an average ratio of 0.55. This is similar to that reported in other studies. The average OC/TC ratio was 0.69 and 0.55 for gasoline-powered and diesel-powered vehicle exhaust as reported by Watson *et al.* (1994). The abundance of Pb was low, ranging from 0.01% to 0.07% in the motor vehicle exhaust profile, which is in contrast to higher Pb abundance (0.1-0.3%) of the profiles taken by Watson and Chow (2001) near the US/Mexico border in 1992 when leaded fuel was still use. In addition, the SO_4^{2-} loading the in motor vehicle exhaust profile was higher than in other profiles in this study.

Comparison of chemical species percentages between GFVE and OFVE are shown in Fig. 2. For most harmful metallic elements, OFVE exhibited higher chemical abundances than GFVE, implying that natural gas was high environmental friendliness in comparison with petroleum products (gasoline and diesel) used as motor vehicles fuel. The most distinct differences were found for EC, which was nearly 8 times as abundant in OFVE relative to GFVE. The differences of Cd and NO_3^- were also large, being nearly 5 and 7 times as abundant in OFVE, respectively. These relative differences in species may be useful in allowing OFVE and GFVE contributions to be distinguished in ambient samples using receptor models.

Enrichment Factor of Geological Sources

In order to obtain an indication regarding the impact of anthropogenic pollution, enrichment factors (EF) of elements for geological sources relative to a soil background were calculated, with Al as the reference element using the following formula:

$$EF = \frac{(X_i/\mathrm{Al})_s}{(X_i/\mathrm{Al})_b} \quad (1)$$

where $(X_i/\mathrm{Al})_s$ and $(X_i/\mathrm{Al})_b$ are ratios of the abundance of element X_i and Al in geological sources and in Chinese background soil (Ministry of Environmental Protection of China, 1990), respectively. As shown in Fig. 3, Cd had high EF for all geological samples, with values ranging from 11 to 123. Pb was enriched in soil dust with an EF of 30 due to the agricultural activities such as fertilization and spraying insecticide (Atafar *et al.*, 2010). Sb exhibited the highest EF for construction derived dust because Sb_2O_3 was used as a white pigment in paints (Jha *et al.*, 2009). Sb was also enriched in road dust with the EF exceeding 10,

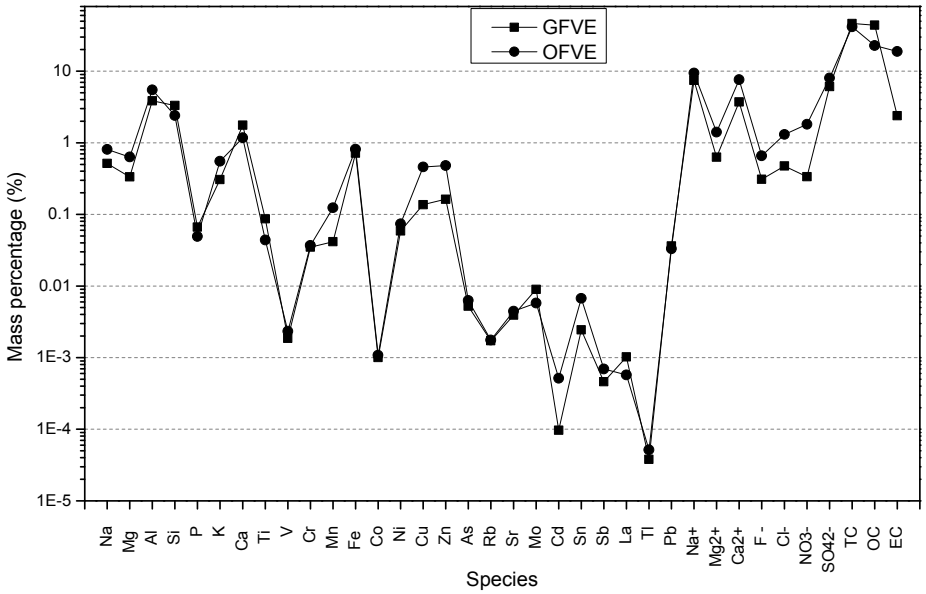

Fig. 2. Comparison of chemical characterization of PM_{10} source profiles between natural gas-powered and gasoline- or diesel-powered vehicle exhaust

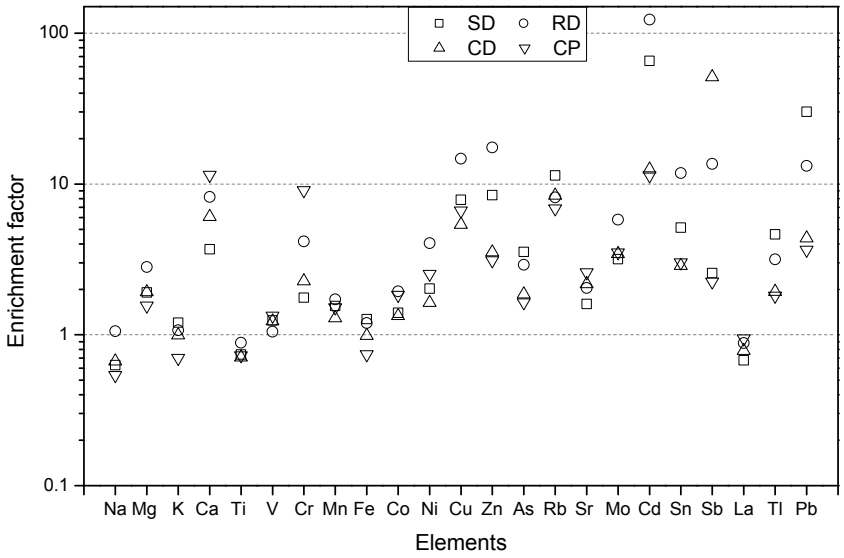

Fig. 3. Enrichment factors of elements in geological dust relative to background soil using Al as the reference element.

suggesting the influence of traffic emissions based on the high EF of Sb in brake lining materials (Voutsa *et al.*, 2002). For the road dust profile, elements including Cu (EF 15) and Zn (EF 17) were also enriched.

Indicator Species for PM_{10} Source Profiles

Many studies have suggested that some specific ratios of species in source profiles could be used for source identification (Cao *et al.*, 2008; Kong *et al.*, 2011a). The following formula was applied to define the indicators of PM_{10} source profiles in Xining (Yang *et al.*, 1998):

$$\text{Ratio}_{j,i} = \frac{(X_i/\Sigma X)_j}{(X_i/\Sigma X)_{\min}} \quad (2)$$

where: X_i is the *i*th individual species abundance; $(X_i/\Sigma X)_j$ is the ratio of *i*th individual species abundance to the sum of all species abundances of source profile j; $(X_i/\Sigma X)_{\min}$ is the ratio of *i*th individual species abundance to the sum of all species abundances that were the minimum of all the source profiles. Normalization of species abundances was used to minimize the effects of physical parameters of species. Normalized individual species abundance was obtained by dividing the *i*th individual species abundance by the sum of *i*th individual species for all the source profiles (Kong *et al.*, 2011a). A higher value of $\text{Ratio}_{j,i}$ signifies that the abundance of *i*th species from emission source j was higher than that from other sources. The highest six ratio values of species for each source profile were recognized as indicator species as listed in Table 3.

In this study, Si, Ca, Ti and Sr were indicator species for all of the geographic sources (SD, RD, CD and CP), except for Rb rather than Ca for SD. Zn has been considered an indicator of SD and RD by others (Kong *et al.*, 2011a). This may reflect geographic differences in the geology, with Qinhai province having a large number of minerals such as celestite containing Sr. EC, considered a marker of incomplete combustion, was identified as an indicator for all fly ash and moter vehical exhaust, except for ISFA. Cd, Si, F^-, Al, Pb and Fe were other indicator species for three industrial fly ash profiles, reflecting differences in industrial production activities. Sr, Cd and Co were markers of CFA. Cu, Ni, Na^+ and the carbon components were markers both of GFVE and OFVE. Mo was a specific marking for GFVE and F^- for OFVE, so these indicators can be used to distinguish between GFVE and OFVE. The differences in indicator species for source profiles in Xining compared to other cities suggests the need for developing source profiles locally.

Comparison of Source Profile with Other Studies

Comparison of the profiles for soil dust, road dust, construction source, coal combustion fly ash and motor vehicle emissions with other studies are shown in Fig. 4.

On the whole, the abundances of crust species such as Al, Si, Ti and Mn in SD and RD in Xining were closer to those reported in other studies than the other species. Most of the ions were higher in SD and RD than in other studies. K^+ was higher in SD here than in other studies. K^+ was one of the key markers for vegetative burning (Watson and Chow, 2001). Therefore, the higher K^+ concentration in SD may be related to the burning of crop straws in Xining. The abundance of Pb in SD in this study was almost 4–20 times that in other studies, also suggesting an effect of agricultural activities.

The CD profile was close to the CP profile in the same area, and different from that profile in other areas, indicating that cement was more used locally. As noted earlier, the lower Pb abundance in motor vehicle emissions in Xining than that in the Imperial and Mexicali Valley was due to the persistent use of Pb in gasoline in Mexico during the period of study.

CONCLUSIONS

Chemical characterization of PM_{10} profiles was carried

out for major emission sources, including soil dust, road dust, construction derived dust, industrial fly ash, coal-fired boilers and motor vehicle exhaust in Xining. The elements were the main components for all of the source

Table 3. Indicator species for major emission sources in Xining.

Source	Indicator species	Source	Indicator species
SD	Si, Rb, Ti, Sr, Al, Tl	EAFA	F^-, EC, Al, Ni, Sb, Na
RD	Ca, Cd, Si, Sr, Ti, K^+	ISFA	Pb, Fe, Tl, Cd, Cl^-, Rb
CD	Sb, Sr, Ca, Si, Ti, Al	CFA	Sr, EC, Cd, Co, Ti, Tl
CP	Ca, Sr, EC, La, Ti, Si	GFVE	OC, EC, Cu, Mo, Ni, Na^+
SFA	EC, Cd, Si, Sr, Ca, K^+	OFVE	EC, Cu, F^-, Ni, Na^+, OC

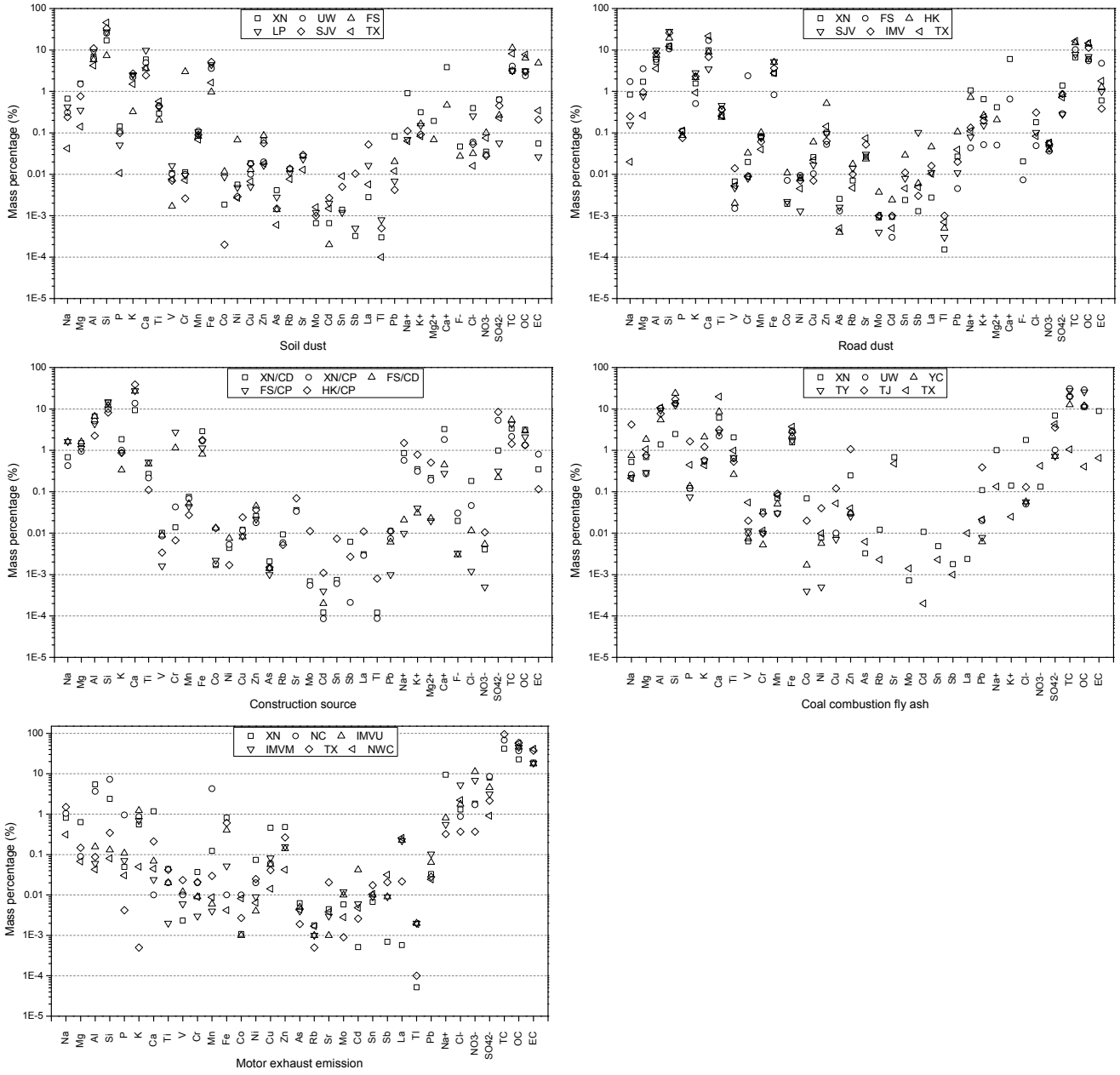

Fig. 4. Comparison of chemical species concentrations of source profiles for Xining and other areas. XN: Xining (this study); UW: Urumqi, YC: Yinchuan, TY: Taiyuan, TJ: Tianjin, NC: northern China (Bi *et al.*, 2007); FS: Fushun (Kong *et al.*, 2011a); LP: Loess plateau (Cao *et al.*, 2008); HK: Hongkong (Ho *et al.*, 2003); SJV: San Joaquin Valley, California (Chow *et al.*, 2003); TX: Texas (Chow *et al.*, 2004); NWC: Northwestern Colorado (Watson *et al.*, 2001); IMV, IMVU, IMVM: Imperial and Mexicali Valleys (in US/Mexico) (Watson and Chow, 2001).

profiles except for motor vehicle exhaust. For motor vehicle exhaust, the carbon components were the most abundance species. Soil dust was dominated by crustal elements such as Si, Al, Ca and Fe. Agricultural activities were responsible for high Pb and OC in soil dust. The road dust profile was silmilar to soil dust, with the most abundance being crustal elements, but high levels of Ca, Zn and EC indicated RD was influenced by construction activities and traffic. The abundance of Sb in CD was 30 times that in CP because of the use of white pigment in buildings paint. Due to the fact that CD is a mixture of cement, sand, paint, etc., the level of SO_4^{2-} was approximately 4 times lower compared with CP. All industrial fly ash was enriched in trace elements including Pb, Cd, Cr, Zn and Ni. However, they differed from each other due to differences in production processes, combustion processes and pollution control devices. Si, Ca, Ca^{2+} and OC were abundant in the ash samples from the silicon plant, while for ash from the electrolytic aluminium plant and iron and steel smelt plant, the dominant species were Al and EC, and Fe, Ca, Ca^{2+} and OC, respectively. The coal-fired boiler profile was dominated by OC, EC, SO_4^{2-}, Ca, Si, Fe and Al species, but was also the main source of other elements including Ti, Co, Sr, Cd, Sb and Tl. OC was the most abundant species in motor vehicle exhaust, accounting for 43.8% and 22.7% of the total accounted mass for GFVE and OFVE, respectively. OFVE exhibited higher chemical abundances for most harmful metallic elements than GFVE, indicating that natural gas is high environmental friendliness in comparison with petroleum products (gasoline and diesel) used as motor vehicles fuel. The large differences in EC, Cd and NO_3^- between OFVE and GFVE may be useful in distinguishing these two sources of vehicle emissions.

The enrichment factors showed that Cd was enriched in all of the geological sources. Pb in soil dust, Sb in construction derived dust and Cu and Zn in road dust were also enriched. The source signatures analysis identified Si, Ca, Sr and Ti as indicators of geological sources, Sr, Cd and Co of the coal-fired source and Cu, Ni, Na^+ and the carbon components of motor vehicle exhausts in Xining. When compared with other studies, Pb and K^+ exhibited higher values for SD in Xining because of the agricultural activities. Differences in source profiles and indicator species between Xining and other cities suggest that source profiles should be developed based on local data and updated frequently. These PM_{10} profiles have now been accepted for source apportionment of atmospheric particulate in Xining to guide air pollution control efforts.

ACKNOWLEDGMENT

This study was funded by the National Basic Research Program of China (2011CB503801) and supported by Qinghai Environmental Monitoring Center (QEMC) of China. The authors are grateful to the staff of QEMC and the students from Nankai University including Bing Lu and Ruojie Zhao for assistance with sampling during the study. Special thanks go to Dr. Wei Li from Nanjing Forestry University, Dr. Marv Johnson from Brigham Young University and Professor Sverre Vedal from the University of Washington who provided language help.

REFERENCES

Aldabe, J., Elustondo, D., Santamaria, C., Lasheras, E., Pandolfi, M., Alastuey, A., Querol, X. and Santamaria, J.M. (2011). Chemical Characterisation and Source Apportionment of $PM_{2.5}$ and PM_{10} at Rural, Urban and Traffic Sites in Navarra (North of Spain). *Atmos. Res.* 102: 191–205.

Atafar, Z., Mesdaghinia, A., Nouri, J., Homaee, M., Yunesian, M., Ahmadimoghaddam, M. and Mahvi, A.H. (2010). Effect of Fertilizer Application on Soil Heavy Metal Concentration. *Environ. Monit. Assess.* 160: 83–89.

Bi, X., Feng, Y., Wu, J., Wang, Y. and Zhu, T. (2007). Source Apportionment of PM_{10} in Six Cities of Northern China. *Atmos. Environ.* 41: 903–912.

Cao, J.J., Chow, J.C., Watson, J.G., Wu, F., Han, Y.M., Jin, Z.D., Shen, Z.X. and An, Z.S. (2008). Size-Differentiated Source Profiles for Fugitive Dust in the Chinese Loess Plateau. *Atmos. Environ.* 42: 2261–2275.

Chen, D., Cheng, S., Zhou, Y., Guo, X., Fan, S. and Wang, H. (2010). Impact of Road Fugitive Dust on Air Quality in Beijing, China. *Environ. Eng. Sci.* 27: 825–834.

Chow, J.C., Watson, J.G., Houck, J.E., Pritchett, L.C., Fred Rogers, C., Frazier, C.A., Egami, R.T. and Ball, B.M. (1994). A Laboratory Resuspension Chamber to Measure Fugitive Dust Size Distributions and Chemical Compositions. *Atmos. Environ.* 28: 3463–3481.

Chow, J.C., Watson, J.G., Ashbaugh, L.L. and Magliano, K.L. (2003). Similarities and Differences in PM_{10} Chemical Source Profiles for Geological Dust from the San Joaquin Valley, California. *Atmos. Environ.* 37: 1317–1340.

Chow, J.C., Watson, J.G., Kuhns, H., Etyemezian, V., Lowenthal, D.H., Crow, D., Kohl, S.D., Engelbrecht, J.P. and Green, M.C. (2004). Source Profiles for Industrial, Mobile, and Area Sources in the Big Bend Regional Aerosol Visibility and Observational Study. *Chemosphere* 54: 185–208.

Davis, S.B. and Wendt, J.O.L. (2000). Quantitative Analysis of High Temperature Toxic Metal Sorption Rates Using Aerosol Fractionation. *Aerosol Sci. Technol.* 33: 536–543.

Fergusson, J.E. and Kim, N.D. (1991). Trace Elements in Street and House Dusts: Sources and Speciation. *Sci. Total Environ.* 100: 125–150.

Gupta, A.K., Karar, K. and Srivastava, A. (2007). Chemical Mass Balance Source Apportionment of PM_{10} and TSP in Residential and Industrial Sites of an Urban Region of Kolkata, India. *J. Hazard. Mater.* 142: 279–287.

Han, B., Bai, Z., Ji, H., Guo, G., Wang, F., Shi, G. and Li, X. (2009). Chemical Characterizations of PM_{10} Fraction of Paved Road Dust in Anshan, China. *Transp. Res. Part D: Transport Environ.* 14: 599–603.

Han, L., Zhuang, G., Cheng, S., Wang, Y. and Li, J. (2007). Characteristics of Re-Suspended Road Dust and Its Impact on the Atmospheric Environment in Beijing. *Atmos. Environ.* 41: 7485–7499.

Ho, K.F., Lee, S.C., Chow, J.C. and Watson, J.G. (2003).

Characterization of PM_{10} and $PM_{2.5}$ Source Profiles for Fugitive Dust in Hong Kong. *Atmos. Environ.* 37: 1023–1032.

Jha, A.K., Prasad, K. and Prasad, K. (2009). A Green Low-Cost Biosynthesis of Sb_2O_3 Nanoparticles. *Biochem. Eng. J.* 43: 303–306.

Kong, S., Han, B., Bai, Z., Chen, L., Shi, J. and Xu, Z. (2010). Receptor Modeling of $PM_{2.5}$, PM_{10} and TSP in Different Seasons and Long-Range Transport Analysis at a Coastal Site of Tianjin, China. *Sci. Total Environ.* 408: 4681–4694.

Kong, S., Ji, Y., Lu, B., Chen, L., Han, B., Li, Z. and Bai, Z. (2011a). Characterization of PM_{10} Source Profiles for Fugitive Dust in Fushun-a City Famous for Coal. *Atmos. Environ.* 45: 5351–5365.

Kong, S., Lu, B., Bai, Z., Zhao, X., Chen, L., Han, B., Li, Z., Ji, Y., Xu, Y., Liu, Y. and Jiang, H. (2011b). Potential Threat of Heavy Metals in Re-Suspended Dusts on Building Surfaces in Oilfield City. *Atmos. Environ.* 45: 4192–4204.

Kong, S., Lu, B., Ji, Y., Zhao, X., Chen, L., Li, Z., Han, B. and Bai, Z. (2011c). Levels, Risk Assessment and Sources of PM_{10} Fraction Heavy Metals in Four Types Dust from a Coal-Based City. *Microchem. J.* 98: 280–290.

Kong, S.F., Lu, B., Ji, Y.Q., Zhao, X.Y., Bai, Z.P., Xu, Y.H., Liu, Y. and Jiang, H. (2012). Risk Assessment of Heavy Metals in Road and Soil Dusts within $PM_{2.5}$, PM_{10} and PM_{100} Fractions in Dongying City, Shandong Province, China. *J. Environ. Monit.* 14: 791–803.

Li, P.H., Han, B., Huo, J., Lu, B., Ding, X., Chen, L., Kong, S.F., Bai, Z.P. and Wang, B. (2012). Characterization, Meteorological Influences and Source Identification of Carbonaceous Aerosols during the Autumn-Winter Period in Tianjin, China. *Aerosol Air Qual. Res.* 12: 283–294.

Li, W. and Bai, Z. (2009). Characteristics of Organic and Elemental Carbon in Atmospheric Fine Particles in Tianjin, China. *Particuology* 7: 432–437.

Li, X., Poon, C.S. and Liu, P.S. (2001). Heavy Metal Contamination of Urban Soils and Street Dusts in Hong Kong. *Appl. Geochem.* 16: 1361–1368.

Ning, D.T., Zhong, L.X. and Chung, Y.S. (1996). Aerosol Size Distribution and Elemental Composition in Urban Areas of Northern China. *Atmos. Environ.* 30: 2355–2362.

Paode, R.D., Shahin, U.M., Sivadechathep, J., Holsen, T.M. and Franek, W.J. (1999). Source Apportionment of Dry Deposited and Airborne Coarse Particles Collected in the Chicago Area. *Aerosol Sci. Technol.* 31: 473–486.

Samara, C., Kouimtzis, T., Tsitouridou, R., Kanias, G. and Simeonov, V. (2003). Chemical Mass Balance Source Apportionment of PM_{10} in an Industrialized Urban Area of Northern Greece. *Atmos. Environ.* 37: 41–54.

Shoubin, F., Gang, T., Gang, L., Yuhu, H., Jianping, Q. and Shuiyuan, C. (2009). Road Fugitive Dust Emission Characteristics in Beijing during Olympics Game 2008 in Beijing, China. *Atmos. Environ.* 43: 6003–6010.

Thorpe, A. and Harrison, R.M. (2008). Sources and Properties of Non-Exhaust Particulate Matter from Road Traffic: A Review. *Sci. Total Environ.* 400: 270–282.

VanCuren, R.A. and Cahill, T.A. (2002). Asian Aerosols in North America: Frequency and Concentration of Fine Dust. *J. Geophys. Res.* 107: AAC 19-1–AAC 19-16,.

Voutsa, D., Samara, C., Kouimtzis, T. and Ochsenkuhn, K. (2002). Elemental Composition of Airborne Particulate Matter in the Multi-Impacted Urban Area of Thessaloniki, Greece. *Atmos. Environ.* 36: 4453–4462.

Waheed, A., Li, X., Tan, M., Bao, L., Liu, J., Zhang, Y., Zhang, G. and Li, Y. (2011). Size Distribution and Sources of Trace Metals in Ultrafine/Fine/Coarse Airborne Particles in the Atmosphere of Shanghai. *Aerosol Sci. Technol.* 45: 163–171.

Watson, J.G., Chow, J.C., Lowenthal, D.H., Pritchett, L.C., Frazier, C.A., Neuroth, G.R. and Robbins, R. (1994). Differences in the Carbon Composition of Source Profiles for Diesel- and Gasoline-Poweredvehicles. *Atmos. Environ.* 28: 2493–2505.

Watson, J.G. and Chow, J.C. (2001). Source Characterization of Major Emission Sources in the Imperial and Mexicali Valleys Along the Us/Mexico Border. *Sci. Total Environ.* 276: 33–47.

Watson, J.G., Chow, J.C. and Houck, J.E. (2001). $PM_{2.5}$ Chemical Source Profiles for Vehicle Exhaust, Vegetative Burning, Geological Material, and Coal Burning in Northwestern Colorado during 1995. *Chemosphere* 43: 1141–1151.

Watson, J.G., Zhu, T., Chow, J.C., Engelbrecht, J., Fujita, E.M. and Wilson, W.E. (2002). Receptor Modeling Application Framework for Particle Source Apportionment. *Chemosphere* 49: 1093–1136.

Wei, B., Jiang, F., Li, X. and Mu, S. (2009). Spatial Distribution and Contamination Assessment of Heavy Metals in Urban Road Dusts from Urumqi, Nw China. *Microchem. J.* 93: 147–152.

Yang, H.H., Lee, W.J., Chen, S.J. and Lai, S.O. (1998). PAH Emission from Various Industrial Stacks. *J. Hazard. Mater.* 60: 159–174.

Yatkin, S. and Bayram, A. (2008). Determination of Major Natural and Anthropogenic Source Profiles for Particulate Matter and Trace Elements in Izmir, Turkey. *Chemosphere* 71: 685–696.

Zhang, W., Zhuang, G., Huang, K., Li, J., Zhang, R., Wang, Q., Sun, Y., Fu, J.S., Chen, Y., Xu, D. and Wang, W. (2010). Mixing and Transformation of Asian Dust with Pollution in the Two Dust Storms over the Northern China in 2006. *Atmos. Environ.* 44: 3394–3403.

Zhao, P., Feng, Y., Zhu, T. and Wu, J. (2006). Characterizations of Resuspended Dust in Six Cities of North China. *Atmos. Environ.* 40: 5807–5814.

Received for review, January 29, 2013
Accepted, September 8, 2013